Analysis of Gibbs Monolayer Adsorbed at the Toluene/Water Interface by UV−Visible Partial Internal Reflection Spectrometry

ARTICLE *in* ANALYTICAL CHEMISTRY · DECEMBER 2006

Impact Factor: 5.64 · DOI: 10.1021/ac061501r · Source: PubMed

9 AUTHORS, INCLUDING:

Takeshi Hasegawa
Kyoto University
116 PUBLICATIONS **1,090** CITATIONS
SEE PROFILE

Tetsuo Okada
Tokyo Institute of Technology
170 PUBLICATIONS **1,916** CITATIONS
SEE PROFILE

Nobuaki Ogawa
Akita University
95 PUBLICATIONS **717** CITATIONS
SEE PROFILE

Sumio Kato
Akita University
40 PUBLICATIONS **163** CITATIONS
SEE PROFILE

Anal. Chem. **2006,** *78,* 7850−7856

Analysis of Gibbs Monolayer Adsorbed at the Toluene/Water Interface by UV−Visible Partial Internal Reflection Spectrometry

Yoshio Moriya,[†] Takeshi Hasegawa,*[,‡,§] Tetsuo Okada,[‡] Nobuaki Ogawa,[†] Erika Kawai,[†] Kosuke Abe,[†] Masataka Ogasawara,[†] Sumio Kato,[†] and Shinichi Nakata[†]

Department of Materials-process Engineering and Applied Chemistry for Environments, Faculty of Engineering and Resource Science, Akita University, 1-1 Tegata Gakuen-machi, Akita 010-8502, Japan, Department of Chemistry, Tokyo Institute of Technology, 2-12-1 Ookayama, Meguro-ku, Tokyo 152-8551, Japan, and PRESTO, Japan Science and Technology Agency, 4-1-8 Honcho, Kawaguchi, Saitama 332-0012, Japan

Gibbs monolayers of lipophilic tetraphenylporphyrinatomanganese(III) and hydrophilic diacid of meso-tetrakis-(4-sulfonatopheny)porphyrin adsorbed at the liquid−liquid interface have been analyzed by UV−visible external reflection (ER) and partial internal reflection (PIR) spectra measured at different angles of incidence. The angle-dependent ER and PIR spectra over the Brewster angles (θ_B^{ER} and θ_B^{IR}) have readily been measured at the toluene/water interface. As preliminarily expected in our previous study, the present study has first proved that the reflection−absorbance of UV−visible PIR spectra quantitatively agrees with the theoretical calculations for the Gibbs monolayer over θ_B^{IR}. In addition, it has also been proved that the absorbance of the PIR spectra is greatly enhanced in comparison to that of the ATR spectra. The enhancement is caused by an optical effect in the monolayer sandwiched between two phases of toluene and water that have different but refractive indices close to each other. This optical enhancement requires an optically perfect contact between the phases, which is difficult to prepare for a solid−solid contact. At the liquid/liquid interface, however, an ideal optical contact is easily realized, which makes the enhancement as much as the theoretical expectation. The PIR spectrometry will be recognized to be a new high-sensitive analytical tool to study Gibbs monolayer at the liquid/liquid interface.

Molecular adsorption and successive chemical reactions at the interface between two immiscible liquids are attractive subjects in many research areas such as solvent extraction, organic synthesis, and molecular recognition in the biological membrane.[1] To elucidate the interface-specific chemical phenomena in the liquid/liquid system, various analytical techniques have been developed in this decade.[2] In particular, time-resolved total internal reflection fluorescence spectroscopy[3] and second harmonic generation (SHG) spectroscopy[4,5] have been used to obtain molecular level information of the liquid/liquid interface. When the interfacial adsorbates are highly absorbing coloration reagents, the polarized UV−visible reflection spectrometry can be employed for the in situ measurements. In the case of the external reflection (ER) spectrometry, the incident light is irradiated obliquely on the interface from the lower refractive index medium to the higher one. In the internal reflection spectrometry, on the contrary, the incident light is irradiated from the higher refractive index medium to the lower one. The internal reflection spectroscopy is further divided into two major optical geometries: the internal total reflection (i.e., attenuated total reflection (ATR)) and partial internal reflection (PIR). The ER and internal reflection techniques are both theoretically expected useful for the measurements of interfacial adsorbates.

We previously compared UV−visible p-polarized PIR (p-PIR) spectra to p-polarized ER (p-ER) ones of an identical chemical species in the J-aggregate form for meso-tetraphenylporphyrin diacid[6] or meso-tetratolylporphyrin diacid[7] at the interface of dodecane and aqueous sulfuric acid. Consequently, it was examined for an angle of incidence higher than the Brewster angle (θ_B^{IR}) that the p-PIR spectrometry yielded both positive and negative bands in a spectrum, which had the same band locations of the corresponding p-ER spectrum, although the band signs in the two spectra were contrary to each other. This is summarized as the "interface selection rule", which indicates that the ER and PIR techniques can be employed complementarily to each other (Table 1). The rules are in short: (1) s-ER spectra give negative bands only, whereas s-PIR spectra give positive bands; (2) the band sign of p-ER and p-PIR spectra alters over Brewster's angles, θ_B^{ER} and θ_B^{IR}, respectively. (θ_B^{IR} is common to PIR and ATR.) Unfortunately, however, it has been difficult to experimentally

* To whom correspondence should be addressed. E-mail: hasegawa@chem.titech.ac.jp.

[†] Akita University.

[‡] Tokyo Institute of Technology.

[§] PRESTO, Japan Science and Technology Agency.

(1) Volkov, A. G., Ed. *Liquid Interfaces in Chemical, Biological, and pharmaceutical Applications*; Marcel Dekker Inc.: New York, 2001.

(2) Tsukahara, S. *Bunseki*, **2005**, (4), 186−191 (in Japanese).

(3) Fujiwara, M.; Tsukahara, S.; Watarai, H. *Phys. Chem. Chem. Phys.* **1999**, *1*, 2949.

(4) Higgins, D. A.; Corn, R. M. *J. Phys. Chem.* **1993**, *97*, 489.

(5) Uchida, T.; Yamaguchi, A.; Ina, T.; Teramae, N. *J. Phys. Chem. B* **2000**, *104*, 12091.

(6) Moriya, Y.; Hasegawa, T.; Hayashi, K.; Maruyama, M.; Nakata, S.; Ogawa, N. *Anal. Bioanal. Chem.* **2003**, *376*, 374.

(7) Moriya, Y.; Nakata, S.; Morimoto, H.; Ogawa, N. *Anal. Sci.* **2004**, *20*, 1533.

10.1021/ac061501r CCC: $33.50
Published on Web 10/17/2006

Table 1. Simplified Interface Selection Rule of the Reflection Spectrometries[a]

optical geometry	angle of incidence	⊥	∥
ER	$0 < \theta_1 < \theta_B^{ER}$	+	−
	$\theta_B^{ER} < \theta_1 < 90°$	−	+
PIR	$0 < \theta_1 < \theta_B^{IR}$	−	+
	$\theta_B^{IR} < \theta_1 < \theta_c$	+	−

[a] The band sign as a function of the angle of incidence (θ_1) and the orientation "directions" to the interface (⊥ and ∥) is summarized for the p-polarization.

Chart 1

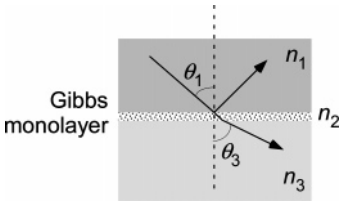

prove and employ these rules quantitatively in particular for the analysis of the liquid/liquid interface, because of the extremely low throughput (reflectivity).

The present paper addresses the incident angle-dependent polarized reflection spectra for the analysis of a lipophilic and hydrophilic porphyrin monolayer adsorbed at the toluene/water interface. In the toluene/water system, the interface reflectivity is relatively high, which makes the low-throughput reflection measurements possible with a relatively good signal-to-noise (S/N) ratio. As a result, the polarized PIR spectrometry has been found most suitable for the high-sensitivity quantitative measurements of the interfacial monolayer. The analytical results will be discussed with respect to optical configurations, chemical status of porphyrin adsorbates, sign and intensity of bands with an angle of incidence (θ_1; defined in phase one; see Chart 1), and analysis of molecular orientation based on the interface selection rule, which aims at employing the PIR spectrometry for the liquid/liquid systems.

EXPERIMENTAL SECTION

Reagents and Chemicals. For the ER measurements, lipophilic 5,10,15,20-tetraphenyl-21*H*,23*H*-porphine manganese(III) chloride (MnTPPCl; Aldrich) was used as a toluene solution. The stock solution was diluted to prepare the initial organic phase with a concentration of 3.2 μM, while the aqueous phase was prepared to be 0.1 M $NaHSO_4$ (pH 1.7). For the PIR and ATR measurements, 5,10,15,20-tetraphenyl-21*H*,23*H*-porphinetetrasulfonic acid (H_2TPPS^{4-} in disulfuric acid tetrahydrate form; Dojindo) and a cationic surfactant cethyltrimethyl ammonium bromide (CTAB) were dissolved in deionized, distilled water with concentrations of 53 and 500 μM, respectively. The aqueous phase was always kept at pH 3.0 by addition of a 1.0 mM HCl aqueous solution, so that the protonated species, H_4TPPS^{2-}, would be retained.

Apparatus and Procedure. Optical arrangements for the variable-angle device were described in detail previously.[6,7] It was designed to perform all the transmission, ER, ATR, and PIR measurements with one device. Optical fibers that accompany a focus lens and a polarizer were assembled on a goniometer, and a cylindrical cell of 2-cm i.d. with a length of 2.55 cm (8 cm^3 in volume) was placed at the center of the optics. The inside of the upper half of the cell was surface-treated with a 5% toluene solution of dimethyldichlorosilane, which made the inner surface hydrophobic, so that the liquid/liquid interface would be made flat when an aliquot (4 cm^3) of aqueous phase and the same volume of organic phase were poured into the cell. UV−visible absorption measurements were carried out by use of an Ocean Optics (Dunedin, FL) USB2000 CCD array spectrometer. The refractive indices of the organic and aqueous media were measured by an Erma Inc. (Tokyo, Japan) Abbe refractometer.

As the first step of the ER measurements, the blank (reference) spectra of the toluene/0.1 M $NaHSO_4$ interface were collected at various angles of incidence with s- and p-polarized UV−visible rays. Then, a slight portion of the toluene phase was replaced by the toluene solution of MnTPPCl, and only the organic phase was gently stirred using a platinum needle to prepare a homogeneous phase with the initial concentration of [MnTPPCl] = 3.2 μM. The ER measurements of the Gibbs monolayer were carried out after attaining the adsorption equilibrium (~5 h) at the corresponding angles and polarizations to those in the blank measurements.

For the PIR measurements, the blank spectra were collected for the toluene/1.0 mM HCl interface. A slight portion of aqueous phase less than 0.2 mL was replaced by the aqueous solution containing H_2TPPS^{4-} and CTAB with a concentration ratio $[CTA^+]/[H_4TPPS^{2-}] = 2$, and only the aqueous phase was gently stirred without disturbing the flat interface to prepare a homogeneous phase that included some ion-pair complexes such as $CTA_2^+-H_4TPPS^{2-}$. The PIR measurements of the Gibbs monolayer were carried out after spending 24 h, so that a stable monolayer would be formed.

Reflection absorbance, A, for all the reflection measurements is commonly defined as $A = \log(R_0/R)$ as a function of wavelength (nm), where R_0 and R are the reflectivities in the absence and presence of the Gibbs monolayer, respectively.

RESULTS AND DISCUSSION

Angle-Dependent ER Spectrum of the Gibbs Monolayer of $MnTPP^+$. Gibbs adsorption of MnTPPCl at the toluene/0.1 M $NaHSO_4$ interface has recently been studied as a pioneer work by Fujiwara and Watarai,[8] in which a polarized UV−visible ER spectrometry with a simple device that we call a "prism cell" was employed.[9,10] The intensity of the negative absorption bands of monomeric adsorbates ($MnTPP^+$) in the s-ER spectra was apparently higher than that of the p-ER spectra at the fixed angle of incidence (70.8°), although the absorbance of the largest band at 480 nm (Soret band) attained only ~ −0.01 for s-polarization even for the saturated monolayer.[8] In the present study, the very weak reflection spectra have readily been measured with the use of our homemade optical device.

Figure 1 presents polarized UV−visible ER spectra observed at several angles of incidence (θ_1) of the $MnTPP^+$ complex monolayer adsorbed at the toluene/0.1 M $NaHSO_4$ interface, in which the initial concentration is [MnTPPCl] = 3.2 μM in the

(8) Fujiwara, K.; Watarai, H. *Bull. Chem. Soc. Jpn.* **2001**, *74*, 1885.
(9) Moriya, Y.; Ogawa, N.; Kumabe, T.; Watarai, H. *Chem. Lett.* **1998**, 221.
(10) Moriya, Y.; Amano, R.; Sato, T.; Nakata, S.; Ogawa, N. *Chem. Lett.* **2000**, 556.

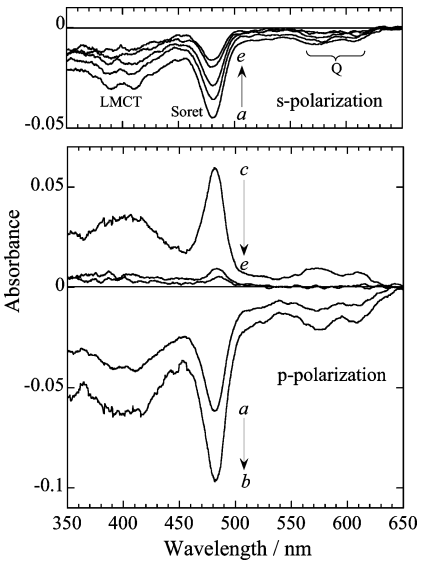

Figure 1. UV−visible s-ER (upper panel) and p-ER (lower panel) spectra of $MnTPP^+$ complex adsorbed at the toluene/0.1 M $NaHSO_4$ (pH 1.7) interface measured by various angles (θ_1) of incidence: a, 30°; b, 43°; c, 53°; d, 66°; e, 70°. [MnTPPCl] = 3.2 μM.

toluene phase. The tendency of the band intensity change with θ_1 clearly agrees with the theoretical expectation, although each of the spectra is a little noisy. In the s-ER spectra presented in the upper panel of Figure 1, all bands appear with negative absorbance and their absolute value (intensity) decreases with increasing θ_1. The negative absorption bands at around 390 and 481 nm are assigned to the ligand to the metal charge transfer (LMCT) band and the Soret band, respectively, and the bands at around 570 and 605 nm are attributed to the two Q-bands.[11]

In the p-ER spectra presented in the lower panel of Figure 1, the spectra a and b measured at low angles of incidence (30° and 43°) exhibit patterns similar to those of s-ER, whereas the spectrum c measured at a high angle of incidence (53°) exhibits a reversed pattern of spectra a and b. In other words, the sign of p-ER band alters over the region $43° < \theta_1 < 53°$, which suggests that θ_B^{ER} would fall in this region. The Brewster angle, θ_B, can roughly be evaluated by eq 1,

$$\theta_B = \tan^{-1}(n_3/n_1) \tag{1}$$

where n_1 and n_3 refer to refractive indices of the incident and transmit phases, respectively, and the monolayer phase (n_2) is not taken into account. The refraction indices $n_1 = 1.345$ for the 0.1 M $NaHSO_4$ phase and $n_3 = 1.493$ for the toluene phase were determined by Abbe refractometer, with which the Brewster angle for the ER geometry in the present system was calculated to be $\theta_B^{ER} = 48°$ that falls in the experimentally expected region.

It is noteworthy that the sign of the LMCT band is always the same as the sign of the Soret band in the angle-dependent p-ER spectra, which suggests that the directions of electron transition moments of chromophores corresponding to these bands are similar to each other with respect to the interface.

Band intensity changes of s- and p-ER spectra at 481 nm as a function of θ_1 are presented in Figure 2 by solid squares and circles, respectively. This plot clearly shows that the s-ER spectra exhibit negative bands only irrespective of θ_1, and the intensity decreases with increasing θ_1, whereas the band of the p-ER spectra changes from negative to positive drastically across θ_B^{ER}. To our best knowledge, no report has been available for angle-dependent polarized UV−visible ER spectra measured for a liquid/liquid system over the Brewster angle, although many measurements of "infrared" ER spectra of a monolayer film on a dielectric substrate[12−15] and on water[16−22] were reported. In the infrared study, the ER spectra were quantitatively analyzed by use of Hansen's approximation formulas.[23] Then, the same technique has been applied to the analysis of the present UV−visible ER spectra of the liquid/liquid interface.

The reflection absorbances for s- and p-polarizations (A_s and A_p) can be calculated by the formulas.[23] When we consider the $x-z$ plane for the incidental plane and the $x-y$ plane for the interface, A_p can be divided into two components for the transition moment oriented perfectly parallel (A_{px}) and perpendicular (A_{pz}) to the interface, respectively:

$$A_s = -\frac{4}{\ln 10}\left(\frac{n_1 \cos\theta_1}{n_3^2 - n_1^2}\right) n_2 \alpha_2 h_2 \tag{2}$$

$$A_{px} = -\frac{4}{\ln 10}\left(\frac{\cos\theta_1/n_1}{\xi_3^2/n_3^4 - \cos^2\theta_1/n_1^2}\right)\left[-\frac{\xi_3^2}{n_3^4}\right] n_2 \alpha_2 h_2 \tag{3}$$

$$A_{pz} = -\frac{4}{\ln 10}\left(\frac{\cos\theta_1/n_1}{\xi_3^2/n_3^4 - \cos^2\theta_1/n_1^2}\right)\left[\frac{n_1^2 \sin^2\theta_1}{(n_2^2 + k_2^2)^2}\right] n_2 \alpha_2 h_2 \tag{4}$$

where $\alpha = 4\pi k/\lambda$ and $\xi_3 = (n_3^2 - n_1^2 \sin^2\theta_1)^{1/2}$.

Here, absorption and extinction coefficients,[24] thickness, and refractive index of the interfacial adsorbates are denoted as α_2, k_2, h_2, and n_2, respectively. Here, the extinction coefficient, k, is defined as the imaginary part of the complex refractive index. For the subscript indices, the reader is referred to Chart 1.

Although Hansen's original equations are based on an optically isotropic model, the divided equations enable us to discuss molecular orientation, since A_{px} and A_{pz} correspond to reflection absorbances of the perfectly oriented transition moments parallel and perpendicular to the surface, respectively.

(11) Grüniger, H.; Möbius, D.; Meyer, H. *J. Chem. Phys.* **1983**, *79*, 3701.
(12) Hasegawa, T.; Umemura, J.; Takenaka, T. *J. Phys. Chem.* **1993**, *97*, 9009.
(13) Hasegawa, T.; Takeda, S.; Kawaguchi, A.; Umemura, J. *Langmuir* **1995**, *11*, 1236.
(14) Brunner, H.; Mayer, U.; Hoffmann, H. *Appl. Spectrosc.* **1997**, *51*, 209.
(15) Mielczarski, J. A.; Mielczarski, E. *J. Phys. Chem.* **1999**, *103*, 5852.
(16) Dluhy, R. A. *J. Phys. Chem.* **1986**, *90*, 1373.
(17) Gericke, A.; Simon-Kutscher, J.; Huehnerfuss, H. *Langmuir* **1993**, *9*, 3115.
(18) Sakai, H.; Umemura, J. *Chem. Lett.* **1993**, (12), 2167.
(19) Flach, C. R.; Brauner, J. W.; Taylor, J. W.; Baldwin, R. C.; Mendelsohn, R. *Biophys. J.* **1994**, *67*, 402.
(20) Ohe, C.; Ando, H.; Sato, N.; Urai, Y.; Yamamoto, M.; Itoh, K. *J. Phys. Chem. B* **1999**, *103*, 435.
(21) Ren, Y.; Kato, T. *Langmuir* **2002**, *18*, 6699.
(22) Kato, N.; Yamamoto, M.; Itoh, K.; Uesu, Y. *J. Phys. Chem. B* **2003**, *107*, 11917.
(23) Hansen, W. N. *Symp. Farady Soc.* **1970**, *4*, 27.
(24) Bertie, J. E Glossary of Terms Used in Vibrational Spectroscopy. In *Handbook of Vibrational Spectroscopy*; Chalmers, J. M., Griffiths, P. R., Eds.; Wiley: Chichester, 2002; Vol. 5, pp 3745−3793.

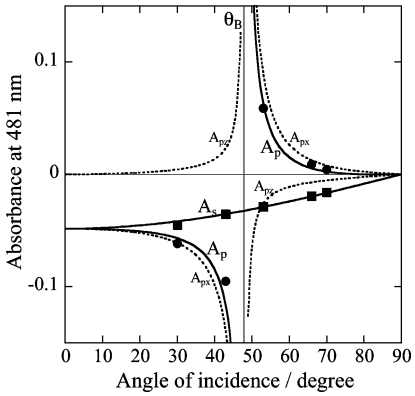

Figure 2. Relationship between the reflection absorbance at 481 nm (Soret band) and the angle of incidence for UV−visible s-ER (solid squares) and p-ER (solid circles) spectra in Figure 1. Simulation curves are calculated by eqs 2−4 with the use of $n_2 = 1.42$, $k_2 = 1.5$, and $n_2\alpha_2 h_2 = 0.0087$.

The plot of the observed absorbance versus θ_1 shown in Figure 2 was analyzed by eqs 2−4, which would provide appropriate values for n_2, k_2, and h_2 at $\lambda = 481$ nm. Simulation curves for A_s and A_p ($= A_{px} + A_{pz}$) drawn by solid lines and those for A_{px} and A_{pz} drawn by dotted lines are presented in the same figure. For the calculation, experimentally determined refractive indices were used: $n_1 = 1.345$ for 0.1 M $NaHSO_4$ and $n_3 = 1.493$ for toluene. After the optimization, it was found that the complex refractive index of the Gibbs monolayer was $n_2 = 1.42$, $k_2 = 1.5$, and $n_2\alpha_2 h_2$ was 0.0087. Although the product, $n_2\alpha_2 h_2$, does not have apparent physical meaning, it is an optimized intermediate value to evaluate the thickness. By considering the wavelength ($\lambda = 481$ nm), h_2 is calculated to be 1.6 Å, which would have a considerable analytical error, since molecular density is not taken into account in the calculation. Therefore, we cannot discuss molecular association with the thickness. It is still impressive, however, that this value falls in the angstrom scale, which suggests that the molecules are not in the perpendicular stance, but they are possibly aligned parallel to the interface as discussed later.

The calculated curves are very close to the observed points in both s- and p-ER cases. In this manner, the drastic band intensity changes across the Brewster angle have quantitatively been proved reasonable. This agreement between the observed and calculated values suggests that the UV−visible ER measurements at the interface are reliable.

One of the reasons for the high-sensitive measurements is the use of toluene, whose refractive index is relatively high among the organic solvents. To compare interface reflectivity (ρ) among various media at a low angle of incidence ($\ll \theta_B^{ER}$), it is convenient to use the simple equation[25] as follows:

$$\rho_s = \rho_p = \left(\frac{n_1 - n_3}{n_1 + n_3}\right)^2 \quad (5)$$

which corresponds to $\theta_1 = 0°$. The calculated interface reflectivities for the systems of air/water, dodecane/4 M H_2SO_4, dodecane/water, and toluene/water, were 0.0249, 0.0003, 0.0010, and 0.0032, respectively. These values indicate that the reflectivity of the liquid/liquid system is far smaller than that of the air/liquid system. Regardless, the reflectivity in the toluene/water system is ~10 times larger than the dodecane/4 M H_2SO_4 system that was studied in our previous works.[6,7] The absorbance enhancement near θ_B^{ER} does not contribute to the high-sensitivity measurements, because the optical throughput (reflectivity) goes close to zero near θ_B^{ER}, which makes the S/N ratio very poor.[14]

According to the interface selection rule of ER[26] (Table 1), the electron transition moment of the chromophore should be oriented rather parallel to the interface when (1) $A_p < 0$ under the condition of $0 < \theta_1 < \theta_B^{ER}$ or (2) $A_p > 0$ under the condition of $\theta_B^{ER} < \theta_1 < 90°$. In a similar manner, it should be oriented rather perpendicular to the interface when (3) $A_p > 0$ under the condition of $0 < \theta_1 < \theta_B^{ER}$ or (4) $A_p < 0$ under $\theta_B^{ER} < \theta_1 < 90°$. The spectra in Figure 2 agree with conditions 1 and 2. This suggests that the pyrrole ring plane in $MnTPP^+$ is oriented nearly parallel to the toluene/0.1 M $NaHSO_4$ interface, which is consistent with the surface-parallel orientation roughly estimated by the analytical thickness of the monolayer discussed above.

Interfacial Adsorption Behavior of H_4TPPS^{2-} with CTA^+. It is known that hydrophilic H_4TPPS^{2-} tends to form a J-aggregate in an acidic aqueous solution with the aid of a coexisting electrolyte[27] or a surfactant.[28] Aggregation itself is also observed in the Gibbs monolayer due to the high-density packing of the adsorbed molecules.[29] For example, the J-aggregation of H_4TPPS^{2-} promoted by a surfactant, CTA^+, at the heptane/water interface has recently been investigated in situ by SHG spectroscopy coupled with circular dichroism (CD) technique.[30] The SHG-CD study revealed that a spiral π-electron delocalization in the excitation of the J-aggregate is caused by π-stacking of TPPS molecules in the aggregate.

In this section, UV−visible PIR spectra of H_4TPPS^{2-} adsorbed with CTA^+ at the interface are discussed. In our study, the toluene/water system has been chosen to prepare the Gibbs monolayer instead of the heptane/water system because the reflectivity is calculated to be more enhanced. Before moving on, the interfacial adsorption behavior and the Gibbs monolayer of ion-pair complexes of $H_4TPPS^{2-}$and CTA^+ should be mentioned.

Absorption spectra of an adequately low-concentration ($\ll 1$ μM) aqueous solution of H_4TPPS^{2-} (with no organic solvent) exhibit the Soret band at 433 nm, which is a characteristic band of a monomer, accompanying two small Q-bands at 592 and 644 nm (data not shown). On the other hand, when a relatively high-concentration solution, 1 μM for example, was measured, the band at 433 nm was decreased in intensity, and instead, new bands related to the J-aggregate of H_4TPPS^{2-} appear at three characteristic positions: 421, 491, and 709 nm.[27] This spectral change was significant particularly when CTA^+ was added to the solution.

Although the band location change from 433 to 421 nm looks like a blue shift, the true characteristic band[27] of the J-aggregates is the band at 491 nm as mentioned in detail later. Therefore, the spectral change suggests that relaxation of Coulomb repulsion

(25) Hecht, E. *Optics*, 2nd ed.; Addison Wesley: Reading, MA, 1987; p 102.

(26) Kattner J.; Hoffmann, H. External Reflection Spectroscopy of Thin Films on Dielectric Substrates. In *Handbook of Vibrational Spectroscopy*; Chalmers, J. M., Griffiths, P. R., Eds.; Wiley: Chichester, 2002; Vol. 3, pp 1009−1027.

(27) Ohno, O.; Kaizu, Y.; Kobayashi, H. *J. Chem. Phys.* **1993**, *99*, 4128.

(28) Maiti, N. C.; Mazumdar, S.; Periasamy, N. *J. Phys. Chem. B* **1998**, *102*, 1528.

(29) Yurizar, Y.; Watarai, H. *Bull. Chem. Soc. Jpn.* **2003**, *76*, 1379.

(30) Fujiwara, K.; Monjushiro, H.; Watarai, H. *Chem. Phys. Lett.* **2004**, *394*, 349.

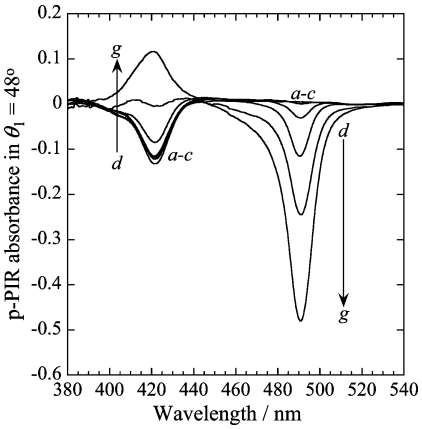

Figure 3. Time-dependent UV−visible p-PIR spectra of H_4TPPS^{2-} monolayer adsorbed at the toluene/water (pH 3.0) interface with $\theta_1 = 48°(>\theta_B^{IR})$ measured at a, 10 min; b, 30 min; c, 1 h; d, 2 h; e, 4 h; f, 8 h; and g, 24 h after the sample preparation. The initial aqueous-phase concentration was $[H_4TPPS^{2-}] = 0.50\ \mu M$, and $[CTA^+]/[H_4TPPS^{2-}] = 2$.

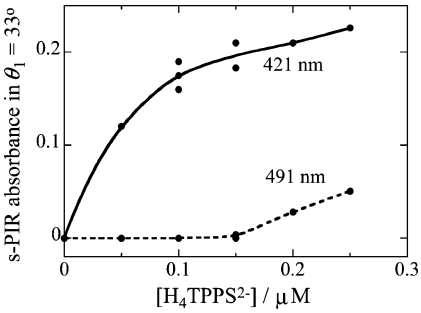

Figure 4. Absorbance changes of the s-PIR spectra with an angle of incidence of 33° at 421 and 491 nm against $[H_4TPPS^{2-}]$ measured after the interfacial adsorption equilibrium with a concentration ratio of $[CTA^+]/[H_4TPPS^{2-}] = 2$.

between H_4TPPS^{2-} ions by addition of CTA^+ is a reason to generate the J-aggregates in the aqueous solution. Although J-aggregates are known to be generated spontaneously in a very thick solution (50 μM for example) with no aid of the surfactant,[31] it has been found that J-aggregates are yielded even in the 1 μM solution by addition of CTA^+.

When toluene is added to the aqueous solution to form a two-phase solution, a part of the J-aggregates is extracted from the aqueous phase and held at the toluene/water interface to form a Gibbs monolayer. UV−visible spectra of the Gibbs adsorbates can be measured by an ATR-like optical configuration with the use of our prism cell device. Here, the toluene and aqueous phases correspond to the first and third phases in Chart 1, respectively, in which the internal reflection occurs in the toluene phase. This configuration was chosen because no absorption band was observed for the toluene phase, whereas some bands due to H_4TPPS^{2-} and J-aggregate were observed for the aqueous phase. Therefore, the adsorbates-specific spectra can be measured by internal reflection spectrometry without interference by absorption bands of the organic bulk phase. In this study, both PIR and ATR measurements were performed below the initial concentration $[H_4TPPS^{2-}] < 1\ \mu M$.

For the internal reflection measurements, the critical angle (θ_c) of the system is available as well as the Brewster angle (θ_B^{IR}), which is calculated by

$$\theta_c = \sin^{-1}(n_3/n_1) \tag{6}$$

Here, θ_B^{IR} in the situation of the internal reflection, θ_B is always smaller than θ_c. In fact, the angles $\theta_B^{IR}(= \tan^{-1}(n_3/n_1))$ and θ_c for PIR of the toluene/water system are calculated to be 42° and 63°, respectively. In addition, the following complementary relationship is known: $\theta_B^{IR} + \theta_B^{ER} = 90°$.[25]

Figure 3 presents time-dependent p-PIR spectra of the interfacial adsorbates in the toluene/water system with an angle of incidence of $\theta_1 = 48°$ that is between θ_B^{IR} and θ_c. The aqueous phase was initially 0.50 μM H_4TPPS^{2-} and 1.0 μM CTA^+. Only one negative absorption band was found at 421 nm after 10 min in Figure 3a. Two hours later, another negative band appeared at 491 nm (Figure 3d), and it grew in the following 24 h, during which the band at 421 nm changed from a negative to a positive band. The final spectrum after attaining equilibrium is presented in Figure 3g, which has a positive band at 421 nm and a negative band at 491 nm. The band at 491 nm is a known characteristic of the J-aggregate adsorbed at the toluene/water interface. This spectral pattern reminds us of the p-PIR spectra of lipophilic tetraphenylporphyrin diacid and tetratolylporphyrin diacid in the J-aggregate form in the dodecane/aqueous sulfuric acid system measured at an angle of incidence greater than θ_B, which were reported in our previous papers.[6,7]

The spectra at an early stage (Figure 3a−c) that give the band at 421 nm with no band at 491 nm are attributed to non-J-aggregated (non-J) species. On the other hand, the spectra Figure 3d−g suggest that non-J species and J-aggregates coexist and their concentration ratio gradually changes in this time region, which is clearly indicated by the drastic changes of the band at 421 nm.

To explore the molecular aggregation status in the monolayer, the concentration dependence of equilibrated interfacial adsorbates was investigated in the concentration range of $0 \le [H_4TPPS^{2-}] \le 0.25\ \mu M$ for the aqueous phase. The molar balance of $[CTA^+]/[H_4TPPS^{2-}]$ was fixed to two. The measurements of s-PIR spectra (data not shown) were performed with an angle of incidence, $\theta_1 = 33°$ ($<\theta_B^{IR}$). The small angle less than θ_B^{IR} was chosen because the s-PIR spectrometry has characteristics as described later that the band sign is always positive regardless of the angle of incidence, and the band intensity becomes larger for a smaller angle of incidence. The observed band intensities at 421 and 491 nm against $[H_4TPPS^{2-}]$ are summarized in Figure 4. The curve of the band at 421 nm reminds us of an adsorption isotherm that exhibits a saturation character.

Here, it is of note that the non-J-specific band at 421 nm is not found for the aqueous bulk phase, while another band instead appears at 433 nm that is assigned to the monomeric species of H_4TPPS^{2-} in the bulk phase. When this blue shift from 433 to 421 nm is considered simply, H-aggregates are expected to be formed in the monolayer. Nevertheless, it is unreasonable that a transition from H-aggregates to J-aggregates occurs when the concentration was increased from nil. It is rather natural to consider that the bands at 421 and 491 nm correspond to the

(31) Ribo, J. M.; Crusats, J.; Farrera, J-A.; Valero, M. L. *J. Chem. Soc., Chem. Commun.* **1994**, 681.

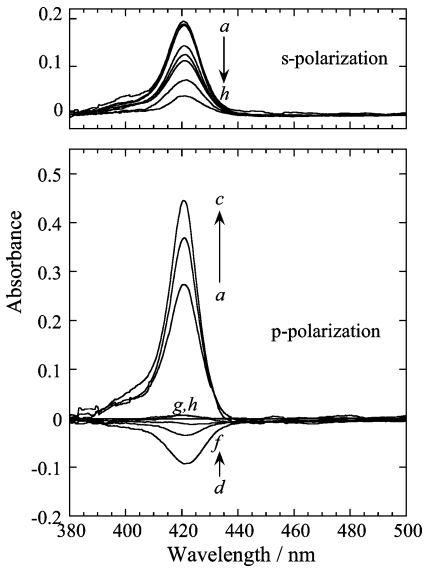

Figure 5. UV−visible s-PIR (upper panel) and p-PIR (lower panel) spectra of non-J species adsorbed at the toluene/water (pH 3.0) interface measured by various angles (θ_1) of incidence: a, 25°; b, 33°; c, 35°; d, 48°; e, 53°; f, 58°; g, 68°; h, 78°. [H_4TPPS^{2-}] = 0.10 μM, [CTA^+]/[H_4TPPS^{2-}] = 2.

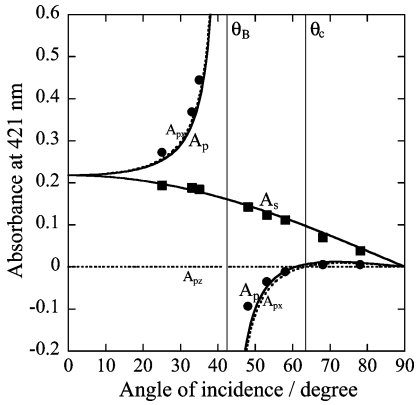

Figure 6. Relationship between the reflection absorbance at 421 nm (non-J species) and the angle of incidence for UV−visible s-PIR (solid squares) and p-PIR (solid circles) spectra in Figure 5. Simulation curves are calculated by eqs 2−4 with the use of $n_2 = 1.42$, $k_2 = 2.5$, and $n_2\alpha_2h_2 = 0.037$.

monomeric (non-J) species and J-aggregates, respectively, so that the results in Figure 4 would be understandable. The reason of the blue shift may be the solvent effect (solvatochromism).[32] Due to the large change of chemical atmosphere about H_4TPPS^{2-} depending on the molecular density in the monolayer, the solvent effect would take place. In short, the dominant species in the low-concentration range is the non-J species, but it accidentally exhibits the blue-shifted band at 421 nm due to the solvent effect.

On the other hand, the absorbance at 491 nm that corresponds to J-aggregate begins to increase above the concentration of 0.15 μM. These analytical results strongly suggests that the non-J species alone is trapped at the interface by Gibbs adsorption when [H_4TPPS^{2-}] < 0.15 μM. When the concentration is larger than 0.15 μM, non-J species and J-aggregates coexist in the interface monolayer. The origin of the J-aggregates is not clear at present, but there are two possibilities: (1) the J-aggregates are from the rearrangement of non-J species in the monolayer and (2) they are from the J-aggregates formed in the aqueous bulk phase.

Angle-Dependent PIR Spectra of H_4TPPS^{2-}. To examine the quantitative accuracy of the PIR technique for the liquid/liquid interface, the angle-dependent PIR spectra have been measured with the initial concentration condition: [H_4TPPS^{2-}] = 0.10 μM. According to the discussion made above, the monomeric (non-J) species would be formed in the monolayer at this concentration.

Figure 5 presents the UV−visible s- (upper panel) and p-polarized (lower panel) spectra of the non-J species adsorbed at the toluene/water interface as a function of θ_1. Since the spectra exhibit no band at 491 nm, no J-aggregates would be available at the interface. Figure 5a−f are PIR spectra measured with the angle of incidence below θ_c, whereas Figure 5g and h are ATR spectra. The band at 421 nm in the s-polarized spectra appears positively, and it decreases with increasing θ_1. In the p-polarized spectra, the absorbance sign alters from positive to negative when the angle was changed over θ_B^{IR} (42°). In addition, the absorbance sign gets back to positive when the angle was changed over θ_c (63°). This means that the measurement modes can continuously be changed from PIR to ATR.

Of note is that the band intensity of the ATR spectra is much smaller than that of the PIR spectra, which holds for both observed and calculated results. The large enhancement of PIR is a result of an optical effect, which happens when an absorbing medium (thin film) is sandwiched between two phases that have different but close refractive indices. In the UV−visible region, the variation of refractive index is much smaller than that in the infrared region, and the situation is suitable for high-sensitivity measurements of the film. Thus far, most of the internal reflection studies have been performed by use of the ATR configuration because of the surface specificity. The present study has revealed, however, that the interfacial adsorbates-specific spectra can be accessed by both ATR and PIR spectrometries quantitatively, and PIR is more preferable in terms of sensitivity. In particular for the analysis of the liquid/liquid system, the UV−visible PIR spectrometry will be recognized to be a powerful tool.

Incident angle-dependent band intensities at 421 nm in s-polarized (solid squares) and p-polarized (solid circles) reflection spectra are plotted in Figure 6. Calculated curves by eqs 2−4 for A_s and A_p (= $A_{px} + A_{pz}$) are also presented in the same figure. The calculation was performed by use of the following optical parameters: $n_1 = 1.493$, $n_2 = 1.42$, $n_3 = 1.334$, $k_2 = 2.5$, and $n_2\alpha_2h_2 = 0.038$, which were obtained by the same procedures mentioned before. It is found that the absorbance changes are readily explained by the theoretical curves. It should be noted that the drastic changes of band sign of A_{px} are theoretically reproduced over the two specific angles, θ_B^{IR} and θ_c, perfectly.

With the optimized parameter product, $n_2\alpha_2h_2$, by parameter fitting, the thickness of the monolayer, h_2, is calculated to be 3.6 Å. As discussed for the $MnTPP^+$ monolayer, the small thickness in the angstrom scale suggests again that the molecules would be aligned nearly parallel to the interface, which is consistent with a fact that the absorbance plot agrees with the A_{px} curve (not A_{pz}). This implies that UV−visible PIR spectrometry is quite useful to discuss the molecular orientation at the liquid/liquid interface.

(32) Takayanagi, M.; Nakata, M.; Ozaki, Y.; Iriyama, K.; Tasumi, M. *J. Mol. Struct.* **1977**, *407*, 85.

CONCLUSION

UV−visible ER, PIR, and ATR spectra have systematically been measured for the analysis of Gibbs monolayer at the liquid/liquid interface. The intensities of the major bands agreed with the theoretical values, and the molecular alignment at the interface has been revealed. It is of note that the different spectrometries with different optical geometries gave consistent analytical results for the monolayer.

As shown by Figure 5, it has been found that the PIR spectrometry is much more suitable than the conventional ATR technique for the analysis of the liquid/liquid interface, since the band intensity is greatly enhanced[33] for both s- and p-polarizations, and the spectra greatly respond to the orientation angle of the transition moment. The present quantitative analysis has clearly proved that the optimum angle of incidence for PIR spectrometry is available less than the Brewster angle under the condition of internal reflection geometry.

(33) Ewing, G. E. *J. Phys. Chem. B* **2004**, *108*, 15953.

ACKNOWLEDGMENT

This work was financially supported by Grant-in-Aid for Scientific Research (B) (T.H.; 16350048) from the Japan Society for the Promotion of Science, and also by The Futaba Electronics Memorial Foundation, Japan.

Received for review August 12, 2006. Accepted September 13, 2006.

AC061501R